Available online at www.sciencedirect.com
ScienceDirect
Planetary and Space Science 56 (2008) 832–835
Planetary and Space Science
www.elsevier.com/locate/pss

Asymmetry of plasma fluxes at Mars. ASPERA-3 observations and hybrid simulations

E. Dubinin[a,*], G. Chanteur[b], M. Fraenz[a], R. Modolo[c], J. Woch[a], E. Roussos[a], S. Barabash[d], R. Lundin[d], J.D. Winningham[e]

[a]MPS, Katlenburg-Lindau, Germany
[b]CETP-IPSL, Velizy, France
[c]IRF-Uppsala, Uppsala, Sweden
[d]IRF, Kiruna, Sweden
[e]SRI, San Antonio, USA

Available online 28 December 2007

Abstract

The asymmetry of fluxes of solar wind and planetary ions is studied by using the ASPERA-3 observations onboard the Mars Express spacecraft in February 2004 to March 2006. Due to the small scale of the Martian magnetosphere and its induced origin, the flow pattern near Mars is sensitive to the directions of the interplanetary magnetic and electric ($-\boldsymbol{V}\times\boldsymbol{B}$) fields. Asymmetry of the magnetic field draping produces an asymmetry in plasma flows in the plane containing the IMF. The crustal magnetic fields on Mars also influence the flow pattern. Scavenging of planetary ions is less efficient in the regions of strong crustal magnetization and therefore the escape fluxes of planetary ions in the southern hemisphere are smaller. The results of the observations are compared to simulations based on a 3D hybrid model with several ion species.

Keywords: Mars; Solar wind; Magnetosphere

The plasma environment at Mars is controlled by the direct interaction between solar wind and planetary exosphere and ionosphere which results in the formation of an induced magnetosphere by draping of the interplanetary magnetic field (IMF) lines around the planet. Therefore the magnetospheric configuration and plasma flows around Mars are governed by the IMF. The forces driving the planetary plasma into motion arise due to the electric field, induced at the solar wind/Mars interaction, and the magnetic field tension of the draped IMF, and, therefore, are also strongly asymmetrical. An asymmetry in the pileup of the IMF was found in the Mars Global Surveyor observations and simulations (Vennerstrom et al., 2003; Bößwetter et al., 2004; Modolo et al., 2005). Morphology and dynamics of plasma flows can also be influenced by the crustal magnetic fields on Mars detected by MGS (Acuña et al., 1998). Thus several factors can produce asymmetries in the plasma distribution near Mars. Among them are a north–south asymmetry induced by the presence of strong crustal sources localized mostly in the southern hemisphere, an asymmetry in planetary ion fluxes due to the action of the interplanetary electric field $\boldsymbol{E}_{\mathrm{IMF}}=-\boldsymbol{V}_{\mathrm{sw}}\times\boldsymbol{B}_{\mathrm{IMF}}$, a draping asymmetry caused by a difference in the magnetic field tension for the spiral IMF configuration. The existence of an asymmetry in fluxes of planetary O^+ ions in the plasma wake of Mars caused by the $\boldsymbol{E}_{\mathrm{IMF}}$ was shown by Barabash et al. (2007). In this paper we focus on another two types of asymmetry. A total of more than 1000 orbits during Feb 2004 – March 2006 of the ASPERA-3 operation onboard the Mars Express spacecraft was analyzed to obtain a statistical pattern of plasma flows around Mars. The ASPERA-3 experiment is a combination of in situ and remote diagnostics of atmospheric escape induced by the solar wind (Barabash et al., 2006). Here we discuss the results obtained from the ELectron Spectrometer (ELS) and Ion Mass Analyzer (IMA). The ELS instrument measures every 4 s 2D

*Corresponding author. Tel.: +49 5556 979 129; fax: +49 5556 979 240.
E-mail address: dubinin@mps.mpg.de (E. Dubinin).

0032-0633/$ - see front matter
doi:10.1016/j.pss.2007.12.006

distributions of the electron fluxes in the energy range of 0.4 eV to 20 keV. The IMA sensor measures 3D-fluxes of different ion species with m/q resolution (m and q are, respectively, mass and electric charge) in the energy range of 10 eV/q to 30 keV/q with a time resolution of $\sim$3 min. We also present some results on an asymmetry of the Martian plasma environment observed in 3D hybrid simulations with multi-ion species (see for details Modolo et al., 2005). Crustal magnetic sources were not included in the model. The parameters of the solar wind plasma and neutral atmospheres are the same as in Modolo et al. (2005). The only important difference is that the angle between the magnetic field and the solar wind velocity was 45° which is more typical for the IMF. Such a configuration creates a draping asymmetry.

The nominal spiral configuration of the IMF at the Mars orbit assumes that the IMF is in the ecliptic plane and has a cone-angle $\alpha = \arctan |B_y|/|B_x| \sim 56°$. An asymmetry in the XY-plane containing the solar wind velocity and the magnetic field vectors may appear since the magnetic field tension forces, which drive the planetary plasma into motion, are different at the dawn and dusk sides. At the dusk side, the IMF draping and the magnetic field tensions are expected to be stronger. Although, the IMF varies significantly it is assumed that in a statistical pattern the IMF vector lies in the $(-X+Y)$ or $(+X-Y)$ sectors and a dawn–dusk asymmetry may be observed. Fig. 1 compares the median distributions of fluxes of the $E_e = 40-60$ eV electrons (top panels) and the proton number density (bottom panels) at the dusk ($Y_{MSO} > 0$) and dawn ($Y_{MSO} < 0$) sides in cylindrical coordinates. Fluxes of the electrons are a good indicator of the plasma boundaries at Mars also due to their higher time resolution (Dubinin et al., 2006). It is observed that the magnetospheric boundary (MB) on the dawn side is more diffuse and a penetration of the sheath plasma into the magnetosphere increases with the distance from Mars.

Figure 2 compares maps of the densities of solar wind protons (top left panel) and planetary oxygen ions (top right panel) in the YZ-plane with the results of hybrid simulations. The density values measured by IMA at $-4R_M < X < 0$ were folded onto one plane and the mean values in each bin were calculated. We only use heavy ion observations inside of the MB to avoid data records influenced by solar wind protons. In hybrid simulations (bottom panels), the upstream magnetic and electric field vectors are in $(+Y-X)$ and $+Z$ directions, respectively. Since newly originated planetary ions in their reference frame feel the motional electric field their motion is strongly asymmetric (Modolo et al., 2005; Bößwetter et al., 2004). To exclude an effect of $\boldsymbol{E}_{\rm IMF}$ the combination of the data with the magnetic field $\boldsymbol{B}_{\rm IMF}$ in the $(-X+Y)$ and $(+X-Y)$ directions was used. We use the same procedure also for the proton fluxes. The observations and simulations show that the dusk side ($Y > 0$) of the induced magnetosphere is stronger screened from the solar wind protons. A shift of the bow shock and 'shocklets' in the sheath in the $+\boldsymbol{B}_{\rm IMF}$ direction is observed in hybrid simulations too. An asymmetry in the planetary ions (top right panel in Fig. 2) is also seen. Most of the oxygen ions occupy the dusk side of the planetary disk with a clear void at the dawn side. A similar effect in the number density of oxygen ions is observed in the simulations.

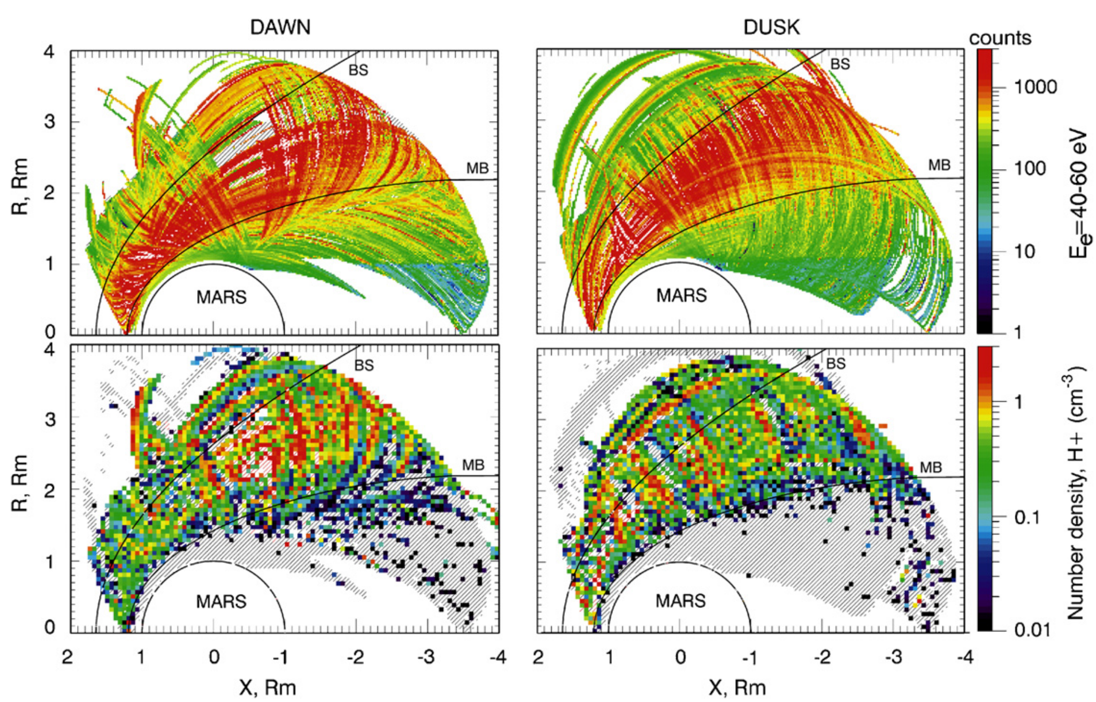

Fig. 1. Maps of the median values of the electron fluxes ($E_e = 40-60$ eV) and the proton number density at the dawn and dusk sides in cylindrical coordinates. Solid curves show the position of the bow shock, BS (Vignes et al., 2000) and induced magnetospheric boundary, MB (Dubinin et al., 2006).

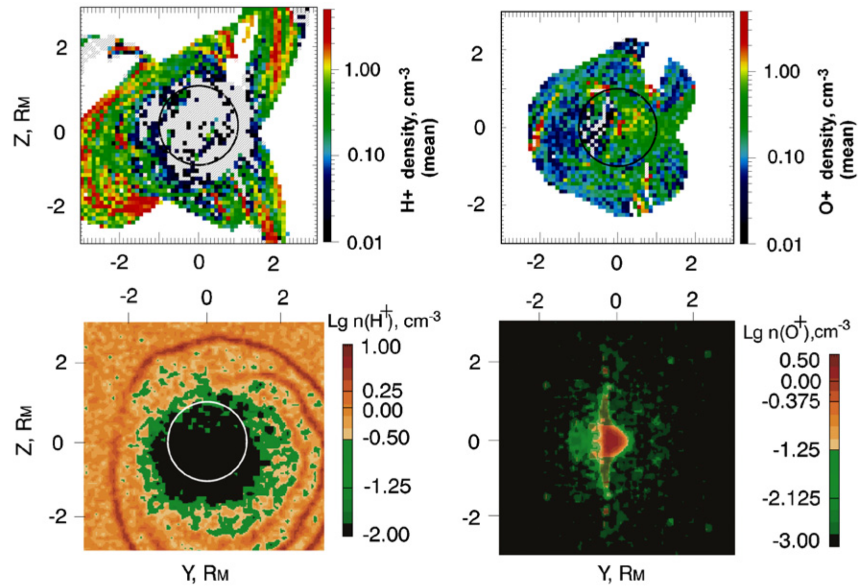

Fig. 2. (Top) Maps of the mean values of the proton and oxygen O^+ ion density in the MSO YZ-plane at the nightsise ($X = -4R_M - 0R_M$). (Bottom) Maps of the number densities of the proton and oxygen ions in the YZ-plane ($X = -1.15R_M$) in the hybrid simulations.

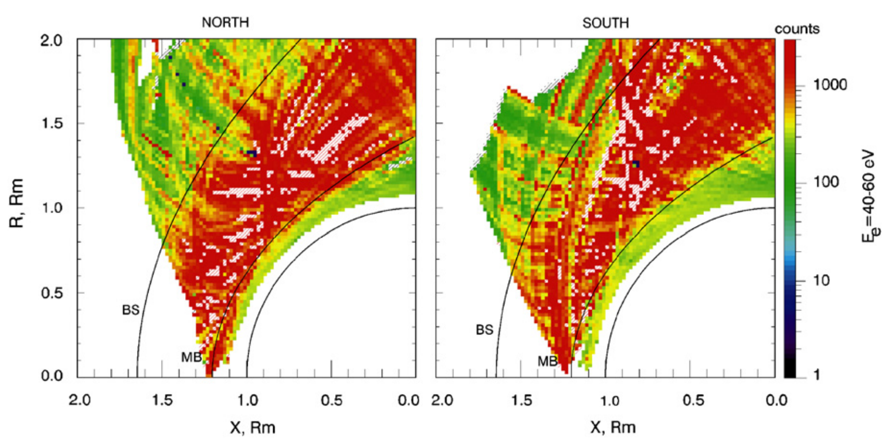

Fig. 3. Maps of the median values of the electron fluxes ($E_e = 40-60$ eV) in the northern and southern hemispheres plotted in cylindrical coordinates.

A possible asymmetry of the proton fluxes caused by crustal magnetic fields is investigated by comparing the observations made in the northern ($Z_{MSO} > 0$) and southern ($Z_{MSO} < 0$) hemispheres. Fig. 3 shows the maps of the median values of the electron fluxes in cylindrical coordinates for both hemispheres. Since the magnetic field of crustal sources strongly decreases with altitude, their contribution to the pressure balance at the MB is expected to be more significant at the dayside. A drop of electron fluxes occurs at larger distances in the southern hemisphere where crustal fields are mainly located although global averaged patterns in both hemispheres are rather similar. A shift at 100–200 km is observed. A sorting of the data by the strength of the crustal field shows that the altitude of the MB increases with the magnetic field value (Fraenz et al., 2006; Dubinin et al., 2006). Another feature which is revealed while analyzing single orbits is related to a local origin of crustal sources. Fig. 4 presents the example of the ASPERA-3 measurements carried out on October 18, 2005. The upper panel shows the spectrogram of electron fluxes. The MEX spacecraft moving along the outbound trajectory at the dayside exits the magnetosphere at ~2252 UT. The exit is accompanied by the appearance of magnetosheath electrons. The solar zenith angle (SZA) and the MEX altitude were ~10° and ~300 km, respectively. At ~2256 UT (SZA ~25°, ALT ~400 km) MEX suddenly again occurs in the ionosphere that is observed by a drop of the solar wind electrons and appearance of typical CO_2 ionospheric peaks at 22–25 eV. At last, at ~2301 UT (ALT ~650 km) the spacecraft finally exits the magnetosphere. The region of a sudden inflation of the magnetosphere coincides with the strong local magnetic field source. The second panel depicts the crustal magnetic field at an altitude of 400 km. The magnetic field value reaches ~60 nT and therefore can deflect the magnetosheath flow and produce a corrugated shape of the boundary.

It is more difficult to observe a north–south asymmetry due to crustal magnetization in fluxes of planetary ions

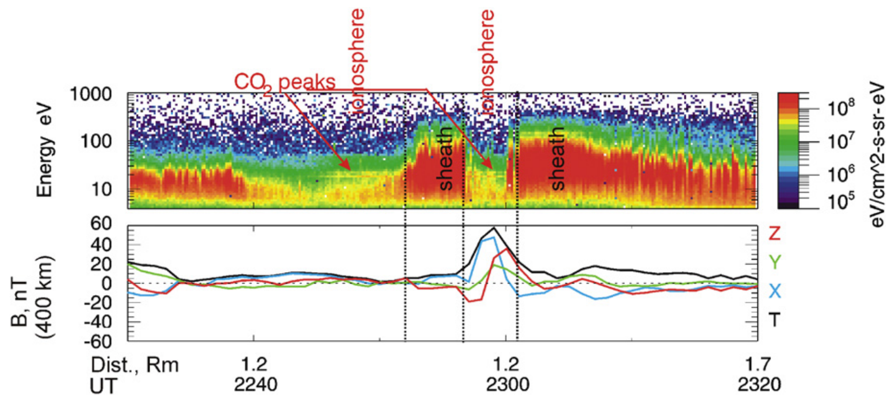

Fig. 4. Spectrogram of electron fluxes and the crustal magnetic field at the altitude 400 km, along the MEX orbit on October 18, 2005.

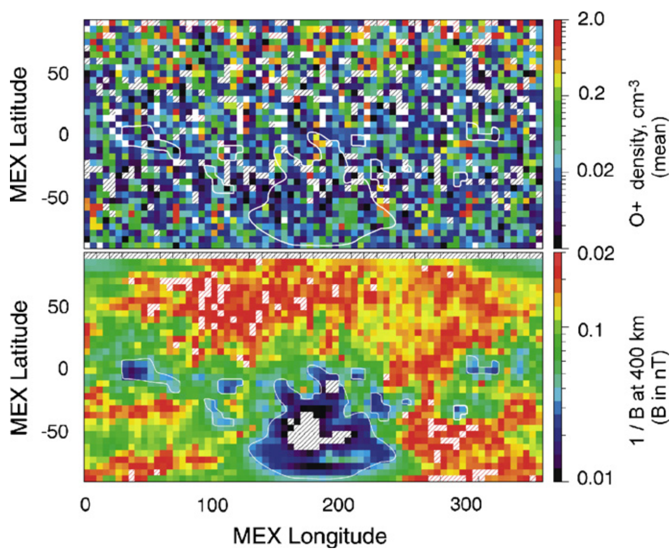

Fig. 5. (Top) Map of the mean values of the oxygen ion density (O^+) as a function of planetocentric eastern longitude and latitude. (Bottom) Inverse of the total crustal field strength (1/nT) at 400 km altitude. The regions of the strongest crustal sources are bounded by the white curves.

since the interplanetary electric field which is directed northward or southward for the nominal spiral IMF can strongly influence a north–south pattern of the ion distribution. Nevertheless assuming that an asymmetry associated with the electric field is strongly canceled due to contributions of opposite signs for the different IMF sectors one can expect to observe an influence of crustal fields on escape processes. Fig. 5 shows the map of the oxygen ion number densities measured in the altitude range of 250–2000 km for SZA $>90^\circ$ as a function of planetocentric latitude and longitude. The bottom panel depicts inverse of the total crustal field strength at 400 km from Connerney et al. (2001). It is observed that the northern hemisphere is a stronger source of planetary ions escaping to the tail. The southern part of the magnetosphere, especially the regions with strongest crustal fields, is better protected from the solar wind induced escape.

In conclusion, ion fluxes in the Martian environment observed by the ASPERA-3 instrument onboard Mars Express show asymmetries due to the IMF draping features and the influence of crustal fields. The 3D multi-ion simulations of the solar wind/Mars interaction used for a comparison with the observations allow display some of these asymmetry features distinctly.

E.D. and M.F. wish to acknowledge Deutsche Forschungsgemeinschaft for supporting this work by Grant WO 910/1-1 and DLR Grants 50QM99035, FKZ 50 QM 0801. E.D. also thanks UVSQ for support of his visit to CETP-IPSL, Velizy, where this work was done. G.C. acknowledges MPS (Lindau, Germany) for the hospitality during his visit. G. C. and R. M. also wish to acknowledge CNES for the support of this study.

References

Acuña, M.H., Connerney, J., Wasilewski, P., et al., 1998. Magnetic field and plasma observations at Mars: initial results of the Mars Global Surveyor MAG/ER experiment. Science 279 (5357), 1676–1680.

Barabash, S., Lundin, R., Andersson, H., et al., 2006. The analyzer of space plasmas and energetic atoms (ASPERA-3) for the European mars express mission. Space Sci. Rev. 126, 113–164.

Barabash, S., Fedorov, A., Lundin, R., Sauvaud, J.-A., 2007. Martian atmospheric erosion rates. Science 315 (5811), 501–503.

Bößwetter, A., Bagdonat, T., Motschmann, U., Sauer, K., 2004. Plasma boundaries at Mars: a 3-D simulation study. Ann. Geophys. 22, 4363–4379.

Connerney, J., Acuña, M.H., Wasilewski, P., et al., 2001. The global magnetic field of Mars and implications for crustal evolution. Geophys. Res. Lett. 28, 4015.

Dubinin, E., Fraenz, M., Woch, J., et al., 2006. Plasma morphology at Mars. ASPERA-3 observations. Space Sci. Rev. 126, 209–238.

Fraenz, M., Winningham, J.D., Dubinin, E., Roussos, E., et al., 2006. Plasma intrusion above Mars crustal fields. Mars Express ASPERA observations. Icarus 182, 406–412.

Modolo, R., Chanteur, G., Dubinin, E., Matthews, A., 2005. Influence of the solar activity on the Martian plasma environment. Ann. Geophys. 23, 433–444.

Vennerstrom, S., Olsen, N., Purucker, M., Acuña, M., 2003. The magnetic field in the pile-up region at Mars, and its variation with the solar wind. Geophys. Res. Lett. 30, 1369.

Vignes, D., Mazelle, C., Reme, H., Acuna, M., et al., 2000. The solar wind interaction with Mars: locations and shapes of the bow shock and magnetic pile-up boundary from the observations of the MAG/ER experiment onboard Mars Global Surveyor. Geophys. Res. Lett. 27, 49–52.